

## Supernova remnants: GMRT based results

Sanjay Bhatnagar

*National Centre for Radio Astrophysics (TIFR), Post Bag No. 3, Ganeshkhind, Pune 411007, India*

### 1. Introduction

Synchrotron radio emission from Supernova remnants (SNRs) emitted by energetic electrons moving in the presence of compressed (and hence amplified) magnetic field has a non-thermal power law dependence on frequency with a negative spectral index  $\alpha$  ( $S \propto \nu^\alpha$ ) making the emission progressively stronger at lower frequencies. Thermal emission from typical HII regions, the other class of objects with extended radio emission in the Galaxy, on the other hand have a flat spectrum above  $\approx 1$  GHz. Below this frequency the optical depth is much greater than 1 and the spectrum turns over with a spectral index of 2. The low frequency continuum spectra of Galactic objects is therefore frequently used to distinguish between thermal and non-thermal sources of emission (Kassim et al., 1989; Kassim and Weiler, 1990; Subrahmanyam and Goss, 1995). The other key observational evidence used to identify SNRs is the morphology. Extended non-thermal sources in the Galaxy with no thermal emission has been the criterion used to identify Galactic sources as SNRs.

About 35% of the SNRs in the catalogue of continuum spectra of some SNRs compiled by Trushkin<sup>1</sup> (Trushkin, 1998) show low frequency free-free absorption by the extended low density warm ionized medium (ELDWIM) in the Galaxy (Kassim, 1989). However, the spectral index of about 40% of SNRs in the comprehensive catalogue of Galactic SNR compiled by Green<sup>2</sup> (Green, 2000) have not been reliably determined. Measurement of this turn-over frequency for SNRs distributed throughout the Galaxy can be used to indirectly measure the distribution of this phase of the ISM, which is otherwise inaccessible to direct observations.

Low frequency continuum mapping in the Galactic plane is therefore important from the point of view of identification of SNRs, for separating thermal from non-thermal emission and for studying the intervening ISM. Taking advantage of the high sensitivity ( $< 10$  mJy/beam) and resolution ( $< 1'$ ) provided by the Giant Meterwave Radio Telescope (GMRT) at low radio frequencies, we have mapped a number of Galactic sources, at 327 MHz (Bhatnagar, 2000).

---

e-mail : [sanjay@ncra.tifr.res.in](mailto:sanjay@ncra.tifr.res.in)

<sup>1</sup>Available from <http://www.ratan.sao.in/cats> on the web

<sup>2</sup>Available from <http://www.mrao.cam.ac.uk/surveys/snrs> on the web

Most of these SNRs were previously classified as candidate SNRs from the surveys done by Gray (1994) using the Molonglo Synthesis Telescope (MOST) at 843 MHz and by Duncan et al. (1997) using the Parkes telescope at 2.4 GHz. Both these observations at relatively high frequencies however suffered from the problems of separating non-thermal emission from thermal emission. At relatively poor sensitivity and resolution ( $\approx 10'$ ), these observations were not sufficient for conclusive identification of these objects as SNRs.

The GMRT at 327 MHz provides a factor 2 lower RMS noise and depending upon the largest baselines used, upto 2-5 times better resolution compared to the observations by Gray and Duncan et al. From these observations, we confirm their identification as SNRs, based on the morphology and non-thermal nature of emission. Resolution in these images is high enough for the study of the brightness variations across the SNR.

## 2. Results

A representative set of 327 MHz-images using the GMRT are presented in this section. The non-thermal spectral index has been derived using the flux densities at a few other frequencies from the literature.

### 2.1 G3.7-0.1

An extended source, just west of G3.7-0.2, seen in the earlier low resolution images, turns out to be a resolved source with shell or barrel morphology. The GMRT 327-MHz image is shown in Fig. 1. This is also in the image of G3.7-0.2 at 1428 MHz published by Gaensler (Gaensler,

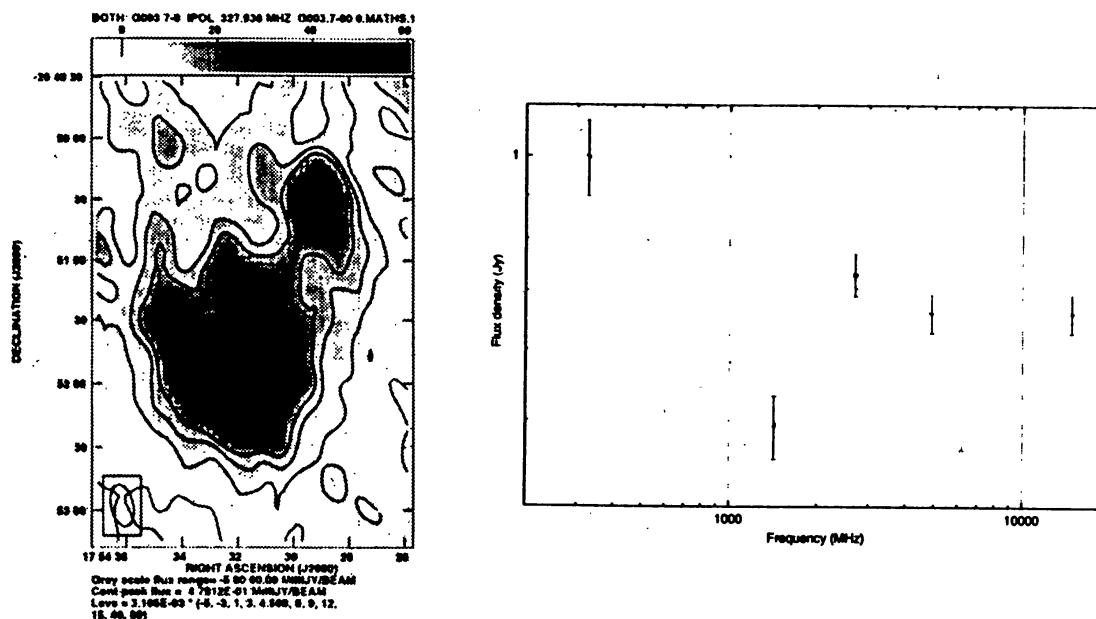


Figure 1. The left panel shows the GMRT 327-MHz of a possibly new shell type small sized SNR G3.7-0.1. The right panel shows the continuum spectra for this source between 327 MHz and 15 GHz. The low frequency spectra is dominated by the non-thermal emission while the flat high frequency spectra is dominated by the line of sight superimposed thermal emission.

1999) at a resolution of  $15'' \times 9''$ . The resolution in the GMRT 327-MHz image is  $20'' \times 12''$ . The size of this source from GMRT image is measured to be  $\approx 1'$  with the centre located at  $RA(2000) = 17^h54^m32^s$ ,  $Dec(2000) = -25^\circ51'130''$ . Another extended source northwest of this source also has a non-thermal spectra and none of these sources are listed in the SNR catalogue (Green, 2000). However there is significant emission in the IRAS  $60\mu m$  image peaking at  $RA_{J2000} = 17^h54^m32^s$ ,  $Dec_{J2000} = -25^\circ50'33''$ .

The continuum spectra shown in Fig. 1, can be modeled as a combination of thermal (detected at  $> 1.4$  GHz) and non-thermal (detected at 327 and 1428 MHz). The shell morphology and detection of non-thermal emission at low frequencies suggests that this is a compact SNR with a line of sight superimposed source of thermal emission.

## 2.2 G4.8+6.2

Fig. 2 shows the GMRT 327-MHz and NVSS 1400-MHz images of G4.8+6.2 (formerly designated as G4.5+6.2). This object of size  $17' \times 18'$  is located  $40'$  east of Kelper's SNR. The total flux density at 327 MHz is  $5.5 \pm 1.2$  Jy. The integrated flux density of G4.8+6.2 at 2.4 GHz was reported to be  $1.3 \pm 0.2$  and the value at 4.85 GHz from Parkes-MIT-NRAO survey (Griffith et al., 1994) (PMN) image of this region was found to be  $1.12 \pm 0.07$  Jy, which gives a spectral index of  $-0.6 \pm 0.1$ .

## 2.3 G356.3-1.5

This SNR is classified as a 'classic barrel' SNR by Gray (Gray, 1994) from the 843-MHz image. The GMRT 327-MHz image, shown in Fig. 3 show the basic structure seen in the 843-MHz image where the two edges are relatively brightened compared to the center of the

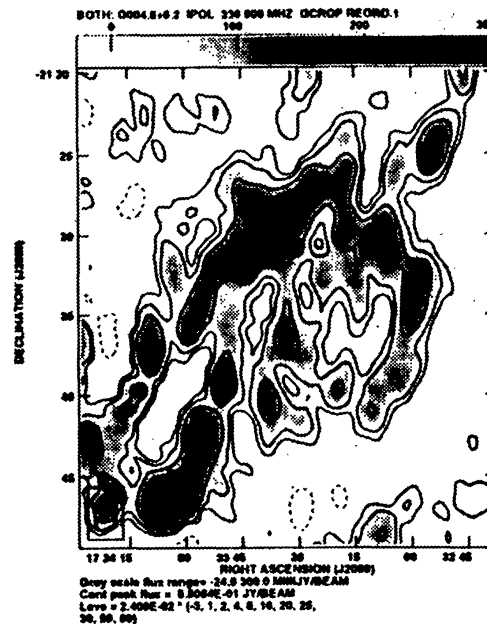


Figure 2. GMRT image of G4.8+6.2 at 327 MHz. The resolution in the image is  $2.2' \times 1.3'$  along PA  $-07^\circ$  and the RMS noise is 23 mJy/beam.

remnant. However, at 327 MHz, the center is also filled with significant emission, not seen in the 843-MHz image. Although it does show the brightened rims, probably of the shell, which were seen as the dominant sources of emission in the 843-MHz image, there is no well defined minima of emission in a direction perpendicular to these rims.

The integrated flux density measured at 332 MHz from GMRT image is  $5.7 \pm 0.2$  Jy. The RMS noise in the image in the vicinity of this object is about 4 mJy/beam. The integrated flux density in the modified image at 843 MHz is reported to be 2.8 Jy. This implies a spectral index of  $-0.74 \pm 0.05$  between 843 and 332 MHz. However the 843-MHz image is marred by a grating response due to G357.7-0.1 and a smooth model of this artifact has been removed, though not entirely successfully (as reported by Gray). The 843-MHz flux density therefore is likely to be underestimated and the resulting spectral index an upper limit.

## 2.4 G356.2+4.5

Fig. 3 shows the GMRT 327-MHz image of G356.2+4.5 where a well defined circular shell of emission of size  $25'$  is evident. The RMS noise in the GMRT map is 10 mJy/beam. Low-level emission is seen projected against the central region. The shell morphology is also clearly visible in the NVSS (Condon et al., 1998) image of this region at 1400 MHz.

The integrated flux density for this SNR at 327 MHz is  $8.1 \pm 1.7$  Jy. The integrated flux density at 2.4 GHz was reported to be  $3.0 \pm 0.3$  Jy and the value at 4.85 GHz from the PMN (Griffith et al., 1994) image was found to be  $1.48 \pm 0.13$  Jy. This gives a spectral index of  $-0.7 \pm 0.2$ .

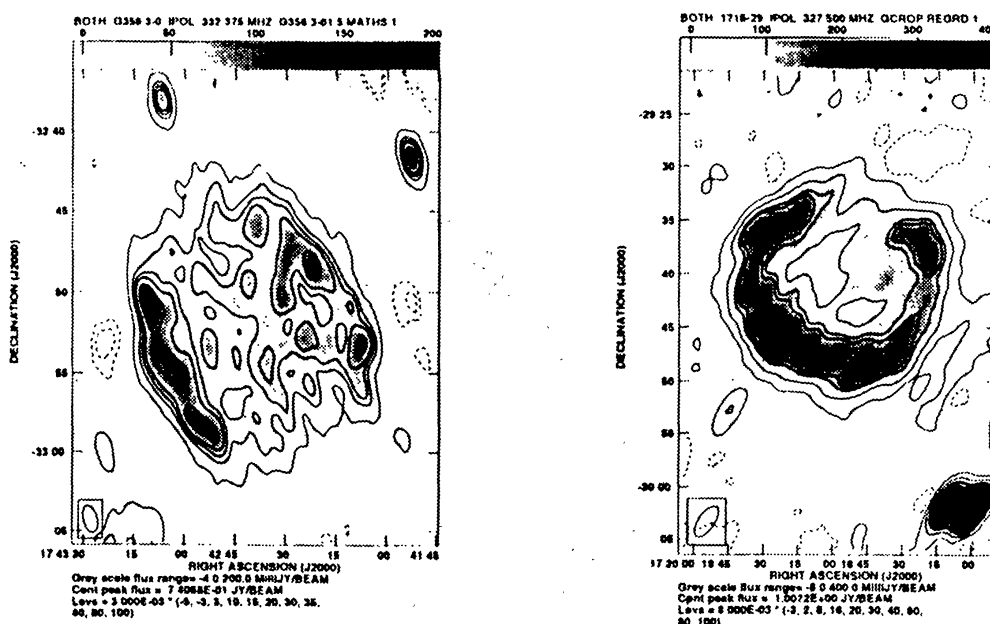


**Figure 3.** GMRT images of G356.3-1.5 and G356.2+4.5 at 327 MHz. The left panel shows the image of the barrel shaped SNR G356.3-1.5. The resolution in the image is  $\approx 1'$  an RMS noise of 4 mJy/beam. The right panel shows the image of G356.2 + 4.5 at resolution of  $3' \times 1.5'$  along PA  $-34^\circ$  and RMS noise of 10 mJy/beam.

## References

- Bhatnagar S., 2000, MNRAS, 327, 453  
Condon J.J., Cotton W.D., Greisen E.W., Yin Q.F., Perley R.A., Taylor G.B., Broderick J.J., 1998, AJ, 115, 1693  
Duncan A.R., Stewart R.T., Haynes R.F., Jones K.L., 1997, MNRAS, 287, 722  
Gaensler B.M., 1999, PhD Thesis, University of Sydney, Australia  
Gray A.D., 1994, MNRAS, 270, 847  
Green D., 2000, A Catalogue of galactic supernova remnants, Mullard Radio Astronomy Observatory, Cavendish Laboratory, Cambridge, UK  
Griffith M.R., Wright A.E., Burke B.F., Ekers R.D., 1994, ApJS, 90, 179  
Kassim N.E., 1989, ApJ, 347, 915  
Kassim N.E., Weiler K.W., 1990, ApJ, 360, 184  
Kassim N.E., Weiler K.W., Erickson W.C., Wilson T.L., 1989, ApJ, 338, 152  
Subrahmanyan R., Goss W.M., 1995, MNRAS, 275, 755-763  
Trushkin S.A., 1998, Spectral Astrophys. Obs., 46, 62-96 (1998), 16:62-96